Single Temperature Sensor Based Evaporator Filling Control Using Excitation Signal Harmonics

Kasper Vinther, Henrik Rasmussen, Roozbeh Izadi-Zamanabadi and Jakob Stoustrup

***Abstract*— An important aspect of efficient and safe operation of refrigeration and air conditioning systems is superheat control for evaporators. This is conventionally controlled with a pressure sensor, a temperature sensor, an expansion valve and Proportional-Integral (PI) controllers or more advanced model based control. In this paper we show that superheat can be controlled without a pressure sensor and without a model of the system. This is achieved by continuous excitation of the system and by applying Fourier analysis, which gives an error signal that can be used together with standard PI control. The proposed method works for systems with "S" shaped input/output maps that satisfy sigmoid function properties and such behavior has been identified in both an air conditioning and a refrigeration system. Tests on these systems show that the superheat can be controlled to a low level over a large operating range with only one sensor. It is believed that the method in general is applicable to a wide variety of nonlinear systems for which the desired operating points are close to points of zero mean curvature of system nonlinearities.**

I. Introduction

Maximization of two-phase refrigerant flow in evaporators is an important aspect of efficient operation of refrigeration and air conditioning systems, because liquid refrigerant accounts for the majority of cooling. At the same time it is important that all refrigerant is vaporized before it enters the compressor to avoid the risk of compressor damage. Control of the evaporator filling level is also known as superheat control, where superheat is the difference between the evaporation temperature and the temperature of the vapor leaving the evaporator. Superheat control is generally achieved using an expansion valve and the most commonly used devices are the Thermostatic Expansion Valve (TXV) and the Electronic Expansion Valve (EEV).

The significant nonlinear response from the opening degree (OD) of the expansion valve to the evaporator superheat poses as a control challenge. TXV's operate well within a certain operating range, but are limited by a constant control gain, which is problematic, since changes in operating conditions for the nonlinear system can cause unstable behavior and actuator hunting [1], [2]. The EEV allows for much greater freedom in expansion valve control and introduces the possibility of using PID control, which is used in the majority of EEV superheat control setups seen today [2]. However, there is still a need for adaption of the controller to changes in operating conditions, which is often solved using some variant of gain scheduling, see e.g. [3].

K. Vinther, H. Rasmussen and J. Stoustrup are with the Section of Automation and Control, Department of Electronic Systems, Aalborg University, 9220, Denmark {kv,hr,jakob}@es.aau.dk

R. Izadi-Zamanabadi is with the Department of Electronic Controllers and Services, Danfoss A/S, 6430, Denmark roozbeh@danfoss.com

There are also alternatives to gain scheduling. In [4] nonlinearity compensation in the valve to superheat response is achieved using a cascaded feedback loop, [5] uses feedback linearization to compensate for nonlinearities and the backstepping design method is used in [6] to find a nonlinear superheat controller that works for a wide range of operating points. Another alternative is to use the compressor, instead of the valve, to control the superheat as done in [7]. There are many possibilities, however, a problem with advanced methods is that they often require a good model of the system, which can be difficult to produce and furthermore each system is often composed of components from many different manufactures making most systems unique. The desire for cheap systems in the industry also means less sensors and thus a need for even more accurate models.

We will in this paper show that the evaporator superheat can actually be controlled over a wide range of operating conditions using only a single temperature measurement at the outlet of the evaporator, thus saving a pressure sensor. Furthermore, this is achieved without using a model of the system and very little a priori system knowledge. Qualitative knowledge about the evaporator nonlinearity from valve input to evaporator outlet temperature is used instead of quantitative knowledge to control the filling of the evaporator. This is possible for Input/Output (I/O) relationships that have sigmoid function properties ("S" shaped I/O map).

The proposed method has taken inspiration from excitation signal based extremum- and slope-seeking control, which are gradient descent non-model based methods (this subject is well covered in e.g. [8]). Extremum-seeking control has e.g. been used in [9] for optimization of condenser water temperature in chilled water cooling plants resulting in a minimization of the total sum of chiller and cooling tower power consumption and in [10] for optimization of air-side economizers in HVAC systems. However, the more general slope-seeking control is better suited for superheat control, since the nonlinear I/O map is "S" shaped and the optimal superheat will be at a certain slope rather than where the slope is zero. A reasonable sub-optimal choice in general is where the slope is largest, since this gives an evaporator outlet temperature that lies between the surrounding temperature and evaporation temperature. However, finding an appropriate reference slope can be very difficult, since this changes with operating conditions and load.

While still using an excitation signal, as in slope-seeking control, we instead propose to use Fourier analysis to calculate an error signal for feedback. We have called this method harmonic control and it is presented in [11]. This is

another approach for single sensor superheat control than the variance based method we presented in [12] and the benefit of harmonic control is that it does not require a system model, it works for a wide operating range, and it does not require any reference set points, which together means that it has a high degree of Plug and Play.

The structure of this paper is as follows. Two different test systems are first introduced in Section II followed by a description of the harmonic control method and simulation results in Section III. Then safety logic is added to the control concept in Section IV and the controller is tested on the two systems with results presented in Section V. Finally, conclusions are drawn in Section VI.

II. System Descriptions

The proposed harmonic controller is designed for systems with steady state I/O maps that exhibit sigmoid function properties and such qualitative behavior has been identified in the relation between the OD of an EEV and the outlet temperature T_o of evaporators in two different refrigeration systems located at Aalborg University (`www.es.aau.dk/projects/refrigeration/`). This behavior is utilized for evaporator filling (superheat) control and the physical layout of the two systems are therefore described in the two following subsections, along with presentation of the qualitative behavior of the evaporator outlet temperature.

A. Air Conditioning System

A simplified schematic of the air conditioning system is presented in Fig. 1. This air conditioning system uses

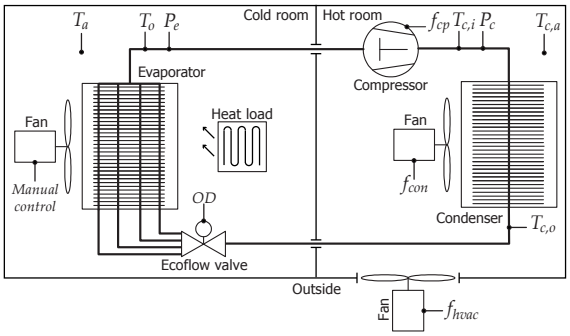

Fig. 1. Simplified schematic of the air conditioning system. T, P and f are indicators for temperature sensors, pressure sensors and frequency control.

refrigerant type R410a and has a finned-tube evaporator with four channels and a cooling capacity of 11 kW. The refrigerant flow is controllable with a Danfoss Ecoflow^{TM}valve. It is possible to control the OD of the valve and the distribution of flow into the individual pipes, however, the distribution is kept constant in this setup. Furthermore, it is possible to control the frequency of both the evaporator and condenser fans, and also the frequency of the fans between the cold room, the hot room and the outside. The scroll compressor frequency is also controllable and sensors measure temperature and pressure at the indicated locations with a sampling interval of 1 second.

A test was conducted on the air conditioning system, where the OD of the valve was gradually increased with 0.01 $\%/s$ from low opening until the refrigerant overflows the evaporator (low superheat). The cold room temperature T_a, the evaporator fan speed, the compressor frequency f_{cp} and the condenser pressure P_c were kept constant during the OD sweep and the test result is shown in Fig. 2. The

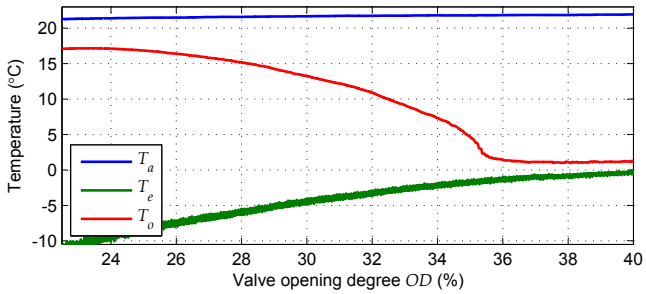

Fig. 2. Evaporator outlet temperature T_o, room air temperature T_a and evaporation temperature T_e during a sweep in OD.

I/O map is almost flat when the valve OD is below 25% and above 37%. Furthermore, it is approximately "S" shaped inbetween, with steepest decline at about 35% OD for the given operating conditions.

B. Refrigeration System

A simplified schematic of the refrigeration system is presented in Fig. 3. This refrigeration system has an evaporator

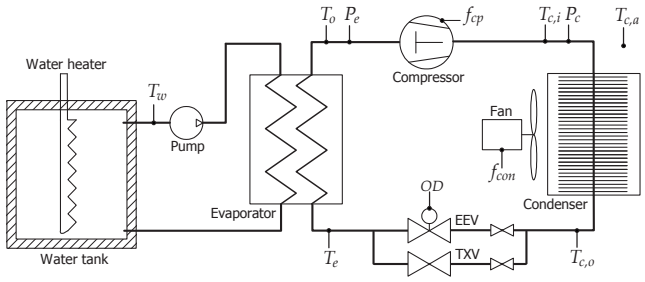

Fig. 3. Simplified schematic of the refrigeration system. T, P and f are indicators for temperature sensors, pressure sensors and frequency control.

with water on the secondary side, which is connected to a water tank with controllable heater and pump. The cooling capacity of the evaporator is 4 kW and the refrigerant type is R134a. It is possible to control the OD of the EEV and the condenser fan frequency. The compressor frequency is again controllable and sensors measure temperature and pressure at the indicated locations with a sampling interval of 1 second.

An OD sweep test was also conducted on the refrigeration system. The water temperature T_w, the pump speed, the compressor frequency f_{cp} and the condenser pressure P_c were again kept constant and the result is shown in Fig. 4. The I/O map is similar to the one shown in Fig. 2, however, with steepest decline at about 80% OD and more "S" shaped. In the following, we will utilize the observed qualitative behavior of the nonlinear I/O map of the two systems, which exhibit sigmoid function properties.

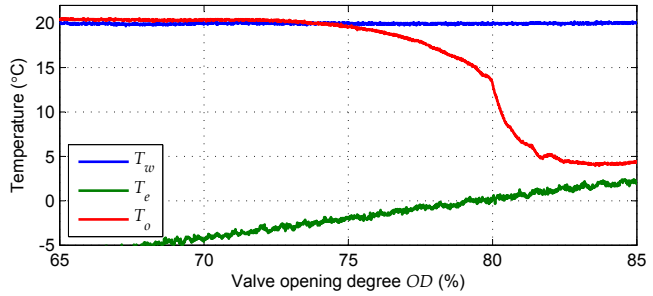

Fig. 4. Evaporator outlet temperature T_o, water temperature T_w and evaporation temperature T_e during a sweep in OD.

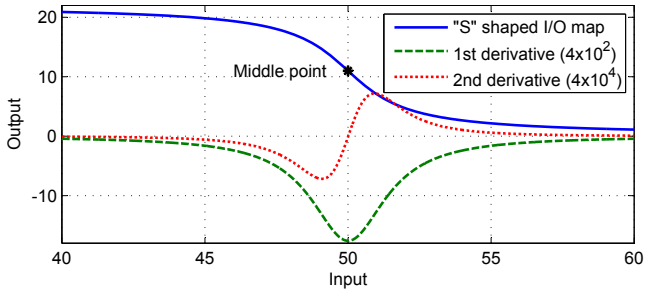

Fig. 5. "S" shaped I/O map (defined in (1)) and corresponding scaled first and second derivative when a ramp is used as input (rate 0.01 per second).

III. Harmonic Control

We have in [11] presented the harmonic control concept. This control concept is intended for systems with a steady state nonlinear "S" shaped I/O map that exhibits sigmoid function properties. A short description of harmonic control is given in the rest of this section and simulations, using the example system defined in (1) and (2), will be given, to show how the method works.

In the following the inverse trigonometric function $atan$ will be used as system nonlinearity. Note, however, that any function with sigmoid function properties could be used. The mathematical expression is

$$y = \left(-atan\left(k_1\frac{(u-k_2)}{k_2}\right)+k_3\right)k_4, \tag{1}$$

where y is the output, u is the input, and the rest ($k_1 = 10\pi$, $k_2 = 50$, $k_3 = \pi/2$, $k_4 = 7$) is arbitrary scaling. This gives the I/O map shown in Fig. 5, where u is limited to values between 0-100 simulating an input saturation, which is seen in most systems. The input $u = 50$ is located in the middle of the "S" shaped curve and this also represents the desired operating point. In addition, first order dynamics with time constant T_{sys} and delay T_d is added;

$$G(s) = \frac{1}{1+sT_{sys}}e^{-sT_d}. \tag{2}$$

The value of T_{sys} and T_d can be chosen almost arbitrarily and are set to 30 and 10 seconds respectively, in the simulation results presented in this paper. The nonlinear gain, input saturation, system time constant and delay are chosen to resemble the characteristics of the evaporator in the refrigeration system shown in Fig. 3.

The basic idea of harmonic control is to exploit the curvature of the nonlinear "S" shaped I/O map. If a ramp signal is used as the input to such an I/O map, then the first derivative is "bell" shaped and the second derivative (indicator of the curvature) is negative and positive respectively to each side of the middle of the "S" shaped I/O map, as shown in Fig. 5. This makes the second derivative usable for feedback, if the middle of the "S" shape is a suitable operating point.

Finding the second derivative of a signal can be problematic due to e.g. measurement noise. The second derivative in the example simulation given above was about 4×10^4 times as small as the measured output. Furthermore, it is also necessary to somehow excite the system to "see" a derivative.

We propose, with the harmonic control method, to continuously excite the system using a sine wave. This makes it possible to indirectly measure the curvature of the I/O map, locally at an operating point, by looking at the distortion of the excitation signal. This distortion is detectable through Fourier analysis, since distortion of a sine wave gives higher order harmonics.

The discrete Fourier series $F(t)$ of a periodic function $f(t)$, sampled at time t_n with sampling time T_{ex}/N, where N is the number of samples in one period T_{ex}, is given as

$$F(t) = a_0 + \sum_{p=1}^{M}\left[a_p cos(p\frac{2\pi}{T_{ex}}t) + b_p sin(p\frac{2\pi}{T_{ex}}t)\right] \tag{3}$$

$$a_0 = \frac{1}{N}\sum_{n=1}^{N} f(t_n)$$

$$a_p = \frac{2}{N}\sum_{n=1}^{N} f(t_n)cos\left(p\frac{2\pi}{N}n\right),\ p = 1, ..., \frac{N}{2}-1$$

$$b_p = \frac{2}{N}\sum_{n=1}^{N} f(t_n)sin\left(p\frac{2\pi}{N}n\right),\ p = 1, ..., \frac{N}{2}-1,$$

where a_p and b_p are the Fourier coefficients for each of the M harmonics denoted by p. These coefficients can be used to calculate a scalar error signal ξ for feedback purposes and a power spectrum density analysis, presented in [11], showed that most of the energy is contained in the first two harmonics. The calculation of a_1, b_1, a_2, and b_2 is performed online in the implementation with time invariant linear FIR filters defined as

$$a_p(k) = \frac{2}{N}\sum_{n=1}^{N} y(k-N+n)cos\left(p\frac{2\pi}{N}n\right),\ p = 1, 2 \tag{4}$$

$$b_p(k) = \frac{2}{N}\sum_{n=1}^{N} y(k-N+n)sin\left(p\frac{2\pi}{N}n\right),\ p = 1, 2, \tag{5}$$

where $y(k)$ is the measured output from the system at time k. Taking the cross product of vectors in $\mathbb{R}^2$ of these coefficients

gives an error signal defined as

$$\xi = \begin{bmatrix} a_1 \\ b_1 \end{bmatrix} \times \begin{bmatrix} a_2 \\ b_2 \end{bmatrix} = a_1 b_2 - a_2 b_1 = |H_1||H_2| sin(\phi) \quad (6)$$
$$|H_1| = \sqrt{a_1^2 + b_1^2}$$
$$|H_2| = \sqrt{a_2^2 + b_2^2},$$

where $|H_1|$ and $|H_2|$ are the amplitudes of the two first harmonics and ϕ is the angle from the first harmonic to the second harmonic. The cross product is a normal vector and it is positive if the operating point is located to the right of the middle point of the "S" shaped nonlinearity and negative to the other side.

It can be a good idea to normalize the error signal ξ, since the amplitude of the excitation signal at the output is dependent on the operating point dependent gain in the system. In (7), the error signal is normalized with the cubed amplitude of the first harmonic, which gives an almost linear feedback signal.

$$\xi_n = \frac{a_1 b_2 - a_2 b_1}{\sqrt{a_1^2 + b_1^2}^3} = \frac{a_1 b_2 - a_2 b_1}{(a_1^2 + b_1^2)^{1.5}}. \quad (7)$$

Other normalizations can be used as well and some of them are shown in Fig. 6. The first three normalized error signals

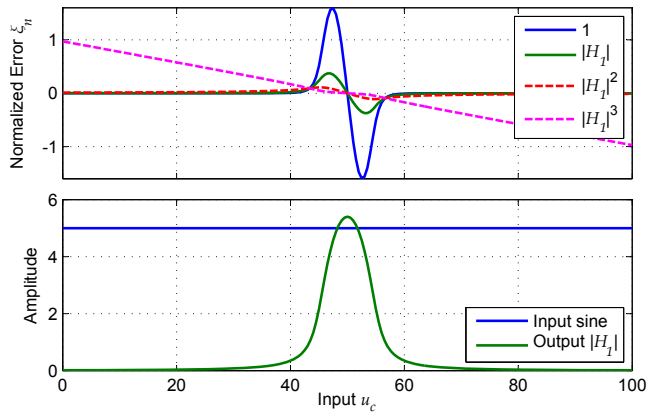

Fig. 6. Four normalizations of the error signal. The error signal is calculated at different offsets in input u_c in steady state and the corresponding amplitude of the first harmonic in the output, together with the amplitude of the input sine.

looks similar to the second derivative in Fig. 5 except for a much larger amplitude (the signal is also flipped, but this depends on the order in the cross product). Another benefit of Fourier analysis is that it is a very powerful way of filtering out unwanted noise, since only the content at the frequencies of the first and second harmonic are considered. The choice of normalization is not important, but can improve the response of the controller. In this simulation example the nonlinearity is quite severe, which is indicated by the amplitude of the excitation signal at the output. This amplitude is very small when the input u_c is below 35 and above 65. In theory this should not matter when using the normalization in (7), however, noise and modeling errors could make the method unstable when the excitation vanishes at the output. Therefore, in some cases it might be better to use e.g. $|H_1|$ or $|H_1|^2$ as normalization, since it better resembles how well the Fourier analysis can be trusted.

After the Fourier analysis and calculation of a normalized error signal, it is now possible to close the loop using e.g. a PI controller. Anti-windup can optionally be added if there is input saturation. Furthermore, it is possible to adapt the amplitude of the input excitation signal using the amplitude of the first harmonic, since a large magnitude improves the Fourier analysis but also disturbs the system more. A healthy balance should be maintained, however, adaption of the excitation signal will not be treated further in this paper (we briefly addressed this issue in [11]). Fig. 7 depicts the proposed harmonic control strategy. The input to the system u is the sum of the input from the control part u_c and the excitation signal u_e and a_e is the amplitude of the excitation signal, which in this paper is considered constant.

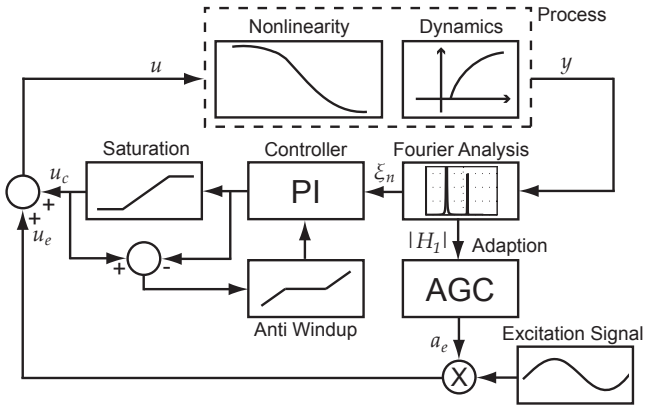

Fig. 7. Harmonic Control Structure. Anti-windup is optional.

The controller has been tested in simulation using the setup shown in Fig. 7 and the system equations defined in (1) and (2). The period of the excitation signal was set to 135 s and the amplitude a_e to 5. Furthermore, the normalization $|H_1|^2$ was used together with PI proportional gain $K_p = 1$, integral time $T_i = 15$ and anti-windup reset time $T_t = T_i/3$. Different starting values of OD (u_c) were used and the result is presented in Fig. 8. The operating point converges to the

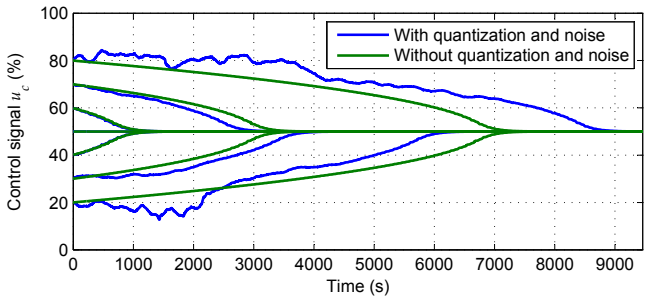

Fig. 8. Simulation results showing closed loop harmonic control applied to the example system given in (1) and (2) for different initial conditions. Input and output quantization (0.2 and 0.1 respectively) and measurement noise ($2\sigma = 0.1$) is added to some of the simulations and the desired operating point is $u_c = 50$.

desired value of $u_c = 50$ in all the simulations, however, the response is more uncertain when noise and quantization is added. This is not surprising, since the amplitude of the harmonics are very small compared to the noise, when the valve OD is below 35% and above 65%, see Fig. 6.

Note that slope-seeking control could not have stabilized the system to the same operating point, because the slope decreases on both sides of the operating point. If slope-seeking control is used, one would have to choose a reference slope that deviates from the middle of the "S" shaped curve, well aware that this slope will be mirrored around the middle of the curve, giving only local stability. Furthermore, choosing a suitable reference can be difficult in itself, since the slope changes when the operating conditions and hence the system nonlinearity changes in the time varying system, giving an unpredictable operating point.

The PI control part of the harmonic controller has been tuned manually in the simulations and tests presented in this paper. However, automatic tuning of the controller will be pursued in future research. When tuning it is important to remember that the Fourier analysis is meant for periodic signals, which means that the controller should not be tuned too aggressively. However, slow variations will only give frequency content in the lower spectrum, which also indicates that the frequency of the excitation should be high. Simulations have also shown that the period of the excitation T_{ex} should approximately be at least twice as large as the combined system time constant T_{sys} and delay T_d.

IV. Safety Logic

Before applying harmonic control to the test systems presented in Section II, some safety logic is added. This logic handles situations when the amplitude of the first harmonic is low, which can give uncertain response as indicated by the simulations shown in Fig. 8. The safety logic is designed to step the valve OD down to a known situation that gives low flow ($u_{c,min}$), when the amplitude of the first harmonic $|H_1|$ gets below a predefined threshold $|H_1|_{t,verylow}$. The control signal u_c is then ramped up, until the amplitude of the first harmonic is larger than a threshold $|H_1|_{t,high}$. However, to speed things up, the information given by the step down in OD can be used to detect if the low amplitude was caused by low flow or overflow in the evaporator. If it was low flow, then the step will not give a noticeable change (more than defined by a threshold $T_{o,t}$) between the temperature before the step $T_{o,old}$ and the new evaporator outlet temperature T_o and the ramp can therefore start at the OD value before the step was made. For added safety, a timer is also implemented, with the purpose of checking if the amplitude $|H_1|$ is consistently lower than a less restrictive threshold $|H_1|_{t,low}$. This will give the controller time to recover by itself, but if it does not do so within a time frame, then recovery is activated automatically. A flowchart giving an overview of the safety logic is presented in Fig. 9.

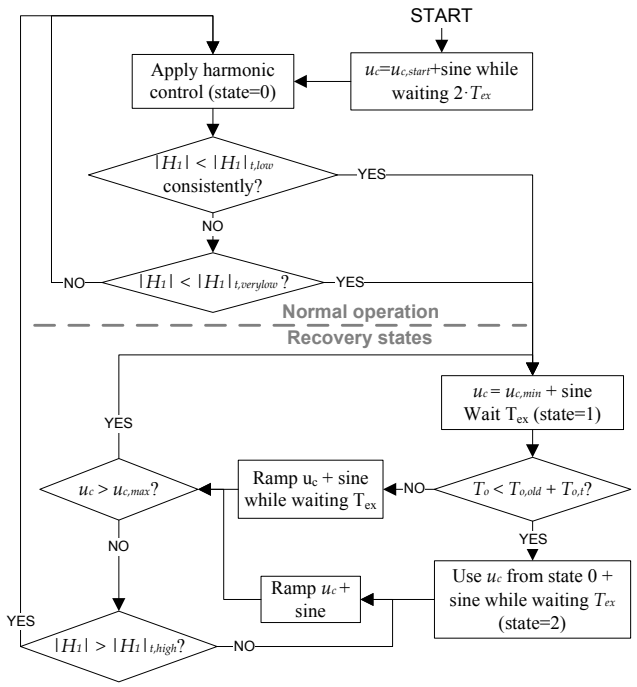

Fig. 9. Flowchart describing the safety logic. State 0 is normal operation (top part of the flowchart), state 1 indicates recovery from overflow situation and state 2 indicates recovery from low flow situation. u_c+sine means that the EEV is applied a control signal u_c superimposed with sine excitation.

V. Test Results

The two systems described in Section II have multiple temperature and pressure sensors, however, the proposed evaporator superheat control only uses the evaporator outlet temperature T_o to control the valve OD. This eliminates the need for a pressure sensor when comparing with conventional control or gives fault tolerant control possibilities.

An 8.33 hour test has been conducted on both systems, where the compressor frequency and heat load was changed in steps according to the test sequence described in [13]. The sequence is also shown in the bottom plot in Fig. 10 and 11. The compressor frequency limits are 35-60 Hz for the refrigeration system and 25-60 Hz for the air conditioning system. In the following it is assumed that the condenser pressure is controlled separately to 9 and 22 bar for the refrigeration system and the air conditioning system, respectively, and that the condenser room temperature is maintained at approximately 22.5 $^\circ C$.

Fig. 10 shows the test result for the refrigeration system, where the controller parameters were set to $T_{ex} = 135$, $a_e = 10$, $K_p = 4$, $T_i = 15$ and $T_t = T_i/3$. These signal parameters gives adequate excitation of the system and the controller is tuned to give a good compromise between convergence speed and robustness towards disturbances. Furthermore, the safety logic parameters where set to $|H_1|_{t,verylow} = 0.5$, $|H_1|_{t,low} = 1.5$, $|H_1|_{t,high} = 2.5$, $T_{o,t} = 4$, $u_{c,min} = 10$, $u_{c,max} = 90$ and ramp rate $= 10/T_{ex}$. Fig. 11 shows the test result for the air conditioning system. The PI parameters were changed to $K_p = 2$ and $T_i = 20$ giving a less aggressive controller and the excitation signal period

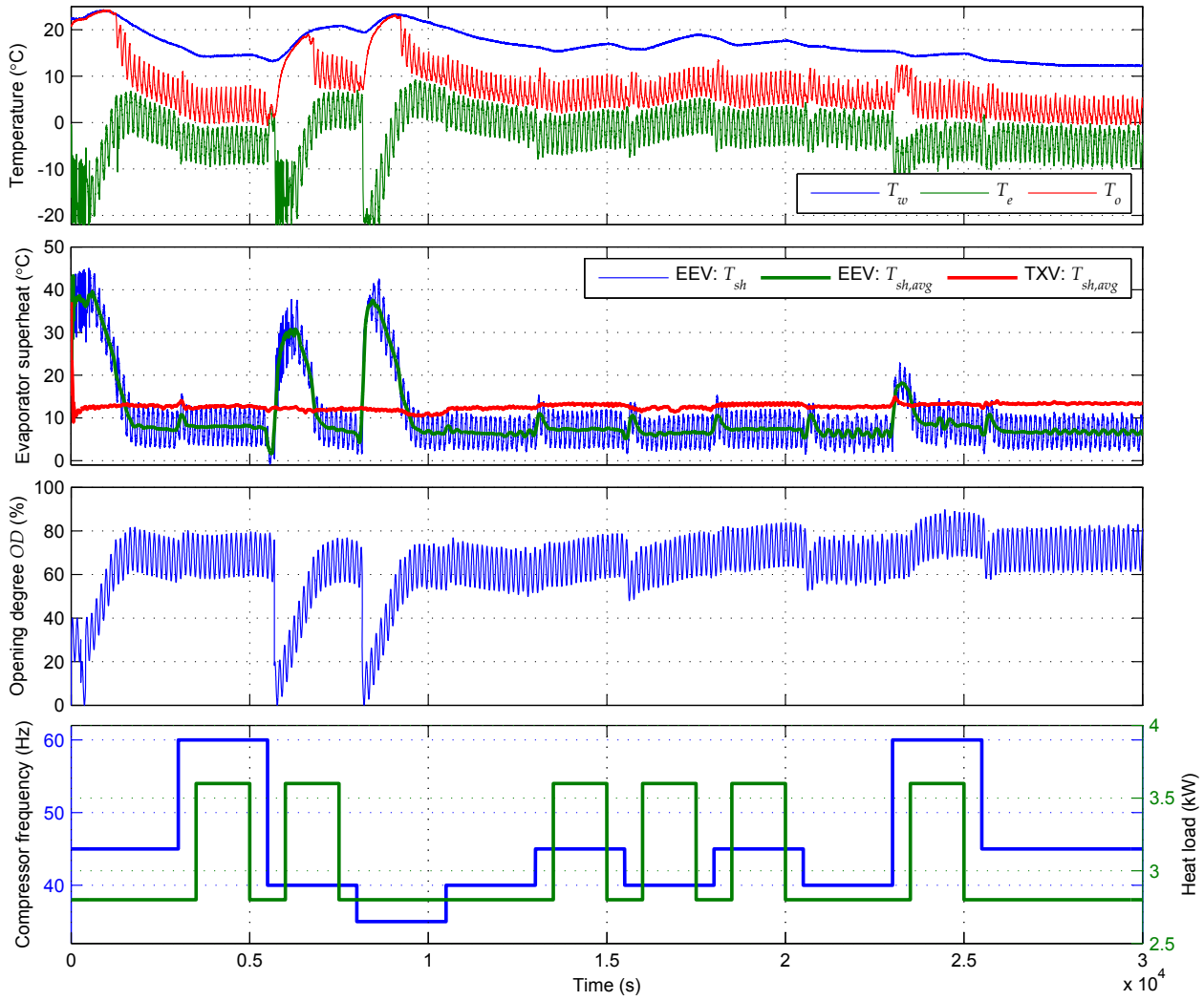

Fig. 10. Test of the harmonic controller on the refrigeration system. The load in the bottom plot is approximately the heat applied to the water tank. The same time scale is used for all four plots. The average superheat achieved with a TXV in a similar test without harmonic control is shown for comparison.

T_{ex} and amplitude a_e were set to 180 and 8 respectively, corresponding to the slightly larger and slower system.

The average superheat was controlled to a low level in both tests using only the evaporator outlet temperature T_o. There are a couple of places where the safety logic is activated. It is also activated in the beginning where the OD is low. This gives faster convergence and means that the controller can be started with a very low OD. All except one activation (going up from lowest compressor frequency in air conditioning system) is caused by evaporator overflow, which gives a very low first harmonic amplitude. The step back in OD causes the superheat to increase and thus gives a performance degradation. However, this mostly happens when there are steps down in compressor frequency and not every time (the timing of the step during the excitation has an effect) and the controller does slowly optimize itself again. The average superheat in the test on the refrigeration system was 10.18 $^{\circ}C$ and only 7.39 $^{\circ}C$ if looking at the time from 10000 to 30000 seconds. This is lower that the average obtained with the TXV, which was 12.68 $^{\circ}C$. Manual fine tuning of the mechanical TXV could potentially have made the superheat lower, however, it could also have been higher depending on the skill of the operator. There are also oscillations in the superheat due to valve hunting when using a TXV, which is comparable to those seen while using continuous excitation and an EEV. However, the superheat oscillations seen in all three tests do not affect the water or room temperature on the secondary side of the evaporator. The average superheat in the test on the air conditioning system was 10.31 $^{\circ}C$.

VI. Conclusion

The proposed non-model based harmonic controller, for nonlinear systems with I/O maps exhibiting sigmoid function properties, have shown, in tests on two different refrigeration systems, that it is possible to control the superheat without a pressure sensor. Furthermore, the method does not require a reference set point and works in a large operating range. The method has shown real Plug and Play potential and convergence can be improved by proper tuning of the PI control parameters, and the amplitude and period of the

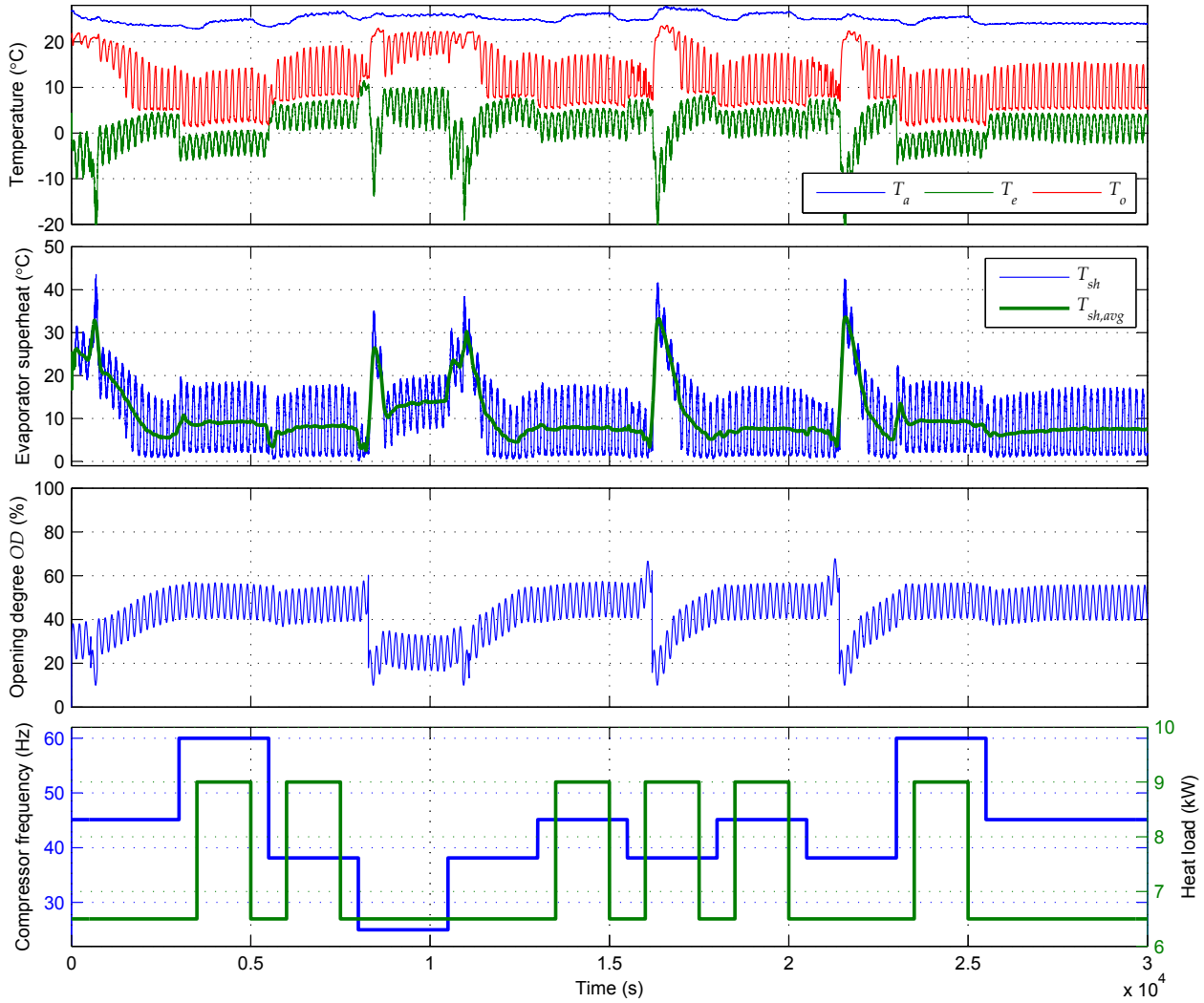

Fig. 11. Test of the harmonic controller on the air conditioning system. The load in the bottom plot is approximately the heat applied to the air conditioned room using an electric heater. The same time scale is used for all four plots.

excitation signal. The speed of the feedback loop is limited by the excitation signal frequency and the method is therefore mostly useful for relatively calm systems. However, there is a big potential in connection with fault tolerant control in case of pressure sensor dropout.

REFERENCES

[1] W. D. Gruhle and R. Isermann, "Modeling and Control of a Refrigerant Evaporator," in *American Control Conference*, Boston, MA, USA, March 1985, pp. 287–292.

[2] D. Lim, B. P. Rasmussen, and D. Swaroop, "Selecting PID Control Gains for Nonlinear HVAC&R Systems," *HVAC&R Research*, vol. 15, no. 6, pp. 991–1019, November 2009.

[3] X.-D. He, S. Liu, H. H. Asada, and H. Itoh, "Multivariable Control of Vapor Compression Systems," *HVAC&R Research*, vol. 4, no. 3, pp. 205–230, February 1998.

[4] M. S. Elliott and B. P. Rasmussen, "On reducing evaporator superheat nonlinearity with control architecture," *International Journal of Refrigeration*, vol. 33, no. 3, pp. 607–614, May 2010.

[5] X.-D. He and H. Asada, "A New Feedback Linearization Approach to Advanced Control of Multi-Unit HVAC Systems," in *American Control Conference*, Denver, CO, USA, June 2003, pp. 2311–2316.

[6] H. Rasmussen and L. F. S. Larsen, "Nonlinear superheat and capacity control of a refrigeration plant," in *Medit. Conference on Control & Automation*, Thessaloniki, Greece, June 2009, pp. 1072–1077.

[7] H. Rasmussen, "Nonlinear Superheat and Capacity Control of a Refrigeration Plant," in *International Conference on Control Applications*, San Antonio, Texas, USA, September 2008, pp. 97–101.

[8] K. B. Ariyur and M. Krstic, *Real-Time Optimization by Extremum-Seeking Control*. Wiley-Interscience, 2003.

[9] H. S. Sane, C. Haugstetter, and S. A. Bortoff, "Building HVAC Control Systems - Role of Controls and Optimization," in *American Control Conference*, Minneapolis, Minn., USA, June 2006, pp. 1121–1126.

[10] P. Li, Y. Li, and J. E. Seem, "Efficient Operation of Air-Side Economizer Using Extremum Seeking Control," *Journal of Dynamic Systems, Measurement, and Control*, vol. 132, no. 3, p. 031009 (10 pages), May 2010.

[11] K. Vinther, H. Rasmussen, R. Izadi-Zamanabadi, and J. Stoustrup, "Utilization of Excitation Signal Harmonics for Control of Nonlinear Systems," in *Multi-conference on Systems and Control*, Dubrovnik, Croatia, October 2012, in press.

[12] K. Vinther, C. H. Lyhne, E. B. Sørensen, and H. Rasmussen, "Evaporator Superheat Control with One Temperature Sensor using Qualitative System Knowledge," in *American Control Conference*, Montreal, Canada, June 2012, in press.

[13] R. Izadi-Zamanabadi, K. Vinther, H. Mojallali, H. Rasmussen, and J. Stoustrup, "Evaporator unit as a benchmark for Plug and Play and fault tolerant control," in *8th IFAC Symposium on Fault Detection, Supervision and Safety of Technical Processes*, Mexico City, Mexico, August 2012, in press.